

# Rabi oscillations and stimulated mode conversion on the subwavelength scale

Xiao Zhang,<sup>1,2</sup> Fangwei Ye,<sup>1,2,\*</sup> Yaroslav V. Kartashov,<sup>3</sup> and Xianfeng Chen<sup>1,2</sup>

<sup>1</sup>Department of Physics and Astronomy, Shanghai Jiao Tong University, Shanghai 200240, China

<sup>2</sup>Key Laboratory for Laser Plasma (Ministry of Education), IFSA Collaborative Innovation Center, Shanghai Jiao Tong University, Shanghai 200204, China

<sup>3</sup>Institute of Spectroscopy, Russian Academy of Sciences, Troitsk, Moscow Region 142190, Russia

\*fangweiy@sjtu.edu.cn

**Abstract:** We study stimulated mode conversion and dynamics of Rabi-like oscillations of weights of guided modes in deeply subwavelength guiding structures, whose dielectric permittivity changes periodically in the direction of light propagation. We show that despite strong localization of the fields of eigenmodes on the scales below the wavelength of light, even weak longitudinal modulation couples modes of selected parity and causes periodic energy exchange between them, thereby opening the way for controllable transformation of the internal structure of subwavelength beams. The effect is reminiscent of Rabi oscillations in multilevel quantum systems subjected to the action of periodic external fields. By using rigorous numerical solution of the full set of the Maxwell's equations, we show that the effect takes place not only in purely dielectric, but also in metallic-dielectric structures, despite the energy dissipation inherent to the plasmonic waveguides. The stimulated conversion of subwavelength light modes is possible in both linear and nonlinear regimes.

©2015 Optical Society of America

OCIS codes: (050.6624) Subwavelength structures; (260.2710) Inhomogeneous optical media

---

## References and links

1. I. I. Rabi, "On the process of space quantization," *Phys. Rev.* **49**(4), 324–328 (1936).
2. X. G. Zhao, G. A. Georgakis, and Q. Niu, "Rabi oscillations between Bloch bands," *Phys. Rev. B Condens. Matter* **54**(8), R5235–R5238 (1996).
3. M. C. Fischer, K. W. Madison, Q. Niu, and M. G. Raizen, "Observation of Rabi oscillations between Bloch bands in an optical potential," *Phys. Rev. A* **58**(4), R2648–R2651 (1998).
4. J. N. Winn, S. Fan, J. D. Joannopoulos, and E. P. Ippen, "Interband transitions in photonic crystals," *Phys. Rev. B* **59**(3), 1551–1554 (1999).
5. R. W. Robinett, "Quantum wave packet revivals," *Phys. Rep.* **392**(1-2), 1–119 (2004).
6. D. Marcuse, *Theory of Dielectric Optical Waveguides* (Academic, 1991).
7. K. O. Hill, B. Malo, K. A. Vineberg, F. Bilodeau, D. C. Johnson, and I. Skinner, "Efficient mode conversion in telecommunication fiber using externally written gratings," *Electron. Lett.* **26**(16), 1270–1272 (1990).
8. K. S. Lee and T. Erdogan, "Fiber mode coupling in transmissive and reflective tilted fiber gratings," *Appl. Opt.* **39**(9), 1394–1404 (2000).
9. Y. V. Kartashov, V. A. Vysloukh, and L. Torner, "Resonant mode oscillations in modulated waveguiding structures," *Phys. Rev. Lett.* **99**(23), 233903 (2007).
10. K. G. Makris, D. N. Christodoulides, O. Peleg, M. Segev, and D. Kip, "Optical transitions and Rabi oscillations in waveguide arrays," *Opt. Express* **16**(14), 10309–10314 (2008).
11. K. Shandarova, C. E. Rüter, D. Kip, K. G. Makris, D. N. Christodoulides, O. Peleg, and M. Segev, "Experimental observation of Rabi oscillations in photonic lattices," *Phys. Rev. Lett.* **102**(12), 123905 (2009).
12. C. D. Poole, C. D. Townsend, and K. T. Nelson, "Helical-grating two-mode fiber spatial-mode coupler," *J. Lightwave Technol.* **9**(5), 598–604 (1991).
13. D. McGloin, N. B. Simpson, and M. J. Padgett, "Transfer of orbital angular momentum from a stressed fiber-optic waveguide to a light beam," *Appl. Opt.* **37**(3), 469–472 (1998).
14. C. N. Alexeyev and M. A. Yavorsky, "Generation and conversion of optical vortices in long-period helical core optical fibers," *Phys. Rev. A* **78**(4), 043828 (2008).
15. C. N. Alexeyev, T. A. Fadeyeva, B. P. Lapin, and M. A. Yavorsky, "Generation of optical vortices in layered helical waveguides," *Phys. Rev. A* **83**(6), 063820 (2011).
16. Y. V. Kartashov, V. A. Vysloukh, and L. Torner, "Dynamics of topological light states in spiraling structures," *Opt. Lett.* **38**(17), 3414–3417 (2013).

17. G. K. L. Wong, M. S. Kang, H. W. Lee, F. Biancalana, C. Conti, T. Weiss, and P. St. J. Russell, "Excitation of orbital angular momentum resonances in helically twisted photonic crystal fiber," *Science* **337**(6093), 446–449 (2012).
18. V. S. Shchesnovich and S. Chávez-Cerda, "Bragg-resonance-induced Rabi oscillations in photonic lattices," *Opt. Lett.* **32**(13), 1920–1922 (2007).
19. B. Terhalle, A. S. Desyatnikov, D. N. Neshev, W. Krolikowski, C. Denz, and Y. S. Kivshar, "Dynamic diffraction and interband transitions in two-dimensional photonic lattices," *Phys. Rev. Lett.* **106**(8), 083902 (2011).
20. J. Takahara, S. Yamagishi, H. Taki, A. Morimoto, and T. Kobayashi, "Guiding of a one-dimensional optical beam with nanometer diameter," *Opt. Lett.* **22**(7), 475–477 (1997).
21. Q. Xu, V. R. Almeida, R. R. Panepucci, and M. Lipson, "Experimental demonstration of guiding and confining light in nanometer-size low-refractive-index material," *Opt. Lett.* **29**(14), 1626–1628 (2004).
22. S. Maier, *Plasmonics: Fundamentals and Applications* (Springer, 2007).
23. F. Ye, D. Mihalache, B. Hu, and N. C. Panoiu, "Subwavelength plasmonic lattice solitons in arrays of metallic nanowires," *Phys. Rev. Lett.* **104**(10), 106802 (2010).
24. C. O. M. S. O. L. Multiphysics, [www.comsol.com](http://www.comsol.com)

## 1. Introduction

Rabi oscillations are the periodic transitions (or revivals) between two stationary states of a quantum system driven by the periodic external field. This is purely resonant effect, whose efficiency strongly depends on the frequency detuning between the external field and own oscillation frequency of the quantum system. Since their prediction by I. Rabi in his seminal paper [1], such revivals and related resonant phenomena have been studied in a variety of atomic, optical, and condensed matter systems [2–5]. Especially fruitful was the extension of the concept of Rabi oscillations to various weakly guiding paraxial optical structures where light propagation is described by the famous Schrödinger equation that also governs the evolution of the wavefunction in quantum-mechanical systems [6–16]. In such paraxial structures, Rabi oscillations manifest themselves as the periodic energy exchange between linear guided modes of the multimode structure, stimulated by weak periodic modulation of the refractive index in the direction of light propagation that plays the role similar to that of the external driving field for multilevel quantum system. Besides purely fundamental aspects, in optical systems the interest to Rabi oscillations is explained by the potential rich practical applications of this effect for the controllable shaping of laser radiation. Rabi oscillations were observed in dynamical long-periodic gratings created in optical fibers [7,8], they were studied in various shallow multimode waveguides [9] and modulated periodic lattices [10,11]. Especially interesting are realizations of Rabi oscillations in the two-dimensional systems, where longitudinal refractive index modulations may couple light modes with different topological charges [12–17]. Notice, that sometimes equations, similar to those describing dynamics of Rabi oscillations, may be encountered in periodic guiding structures without any longitudinal variations [18,19].

So far, the dynamics of optical Rabi oscillations was analyzed mostly in the paraxial multimode guiding structures, where all characteristic scales (beam and waveguide widths) substantially exceed the wavelength. In this case the coupled-mode approach applied to the Schrödinger equation, governing light evolution, yields equations for mode amplitudes analogous to those for populations of levels in a driven quantum system. On the other hand, last decade has witnessed rapid advances in nanotechnologies that already allow fabrication of optical waveguides with subwavelength dimensions [20,21]. Considerable waveguide depths can be achieved (strong guiding regime), so that eigenmodes of such structures also become subwavelength. Especially fruitful is the combination of dielectrics and metals allowing to confine light due to the excitation of surface plasmon polaritons (SPPs) [22]. In such structures one has to resort to solution of the full set of Maxwell's equations, since the paraxial approximation fails to describe light evolution. A general question arises – are Rabi oscillations possible in the modulated subwavelength structures and to which extent this effect can be used for shaping of narrow light beams?

In this paper we address Rabi oscillations in subwavelength dielectric and metal-dielectric waveguides and show that this effect persists at the subwavelength scales and can be used to control the modal structure of the output beams. Longitudinal modulation of the dielectric permittivity in the waveguide region results in a highly selective excitation of modes of proper parity, while efficiency of this process is controlled by the detuning of modulation frequency from the resonant value. Efficient mode conversion can be achieved at very short propagation distances  $\sim 20 \mu\text{m}$ .

## 2. The model and coupled mode theory

We consider the propagation of a TM-polarized light beam along the  $z$ -axis of a subwavelength waveguide with longitudinally modulated dielectric permittivity. The evolution of nonzero components of the electric  $\mathbf{E} = (E_x, 0, E_z)$  and magnetic  $\mathbf{H} = (0, H_y, 0)$  fields for selected polarization state is governed by the reduced system of Maxwell's equations:

$$\begin{aligned} i \frac{\partial E_x}{\partial z} &= -\frac{1}{\varepsilon_0 \omega} \frac{\partial}{\partial x} \left[ \frac{1}{\varepsilon(x, z)} \frac{\partial H_y}{\partial x} \right] - \mu_0 \omega H_y, \\ i \frac{\partial H_y}{\partial z} &= -\varepsilon_0 \varepsilon(x, z) \omega E_x, \end{aligned} \quad (1)$$

where we have excluded the longitudinal component  $E_z = [i / \varepsilon_0 \varepsilon(x, z) \omega] \partial H_y / \partial x$  of the electric field for convenience;  $\varepsilon_0$  and  $\mu_0$  are the vacuum permittivity and permeability; and  $\omega$  is the frequency of light. The function  $\varepsilon(x, z)$  describes the relative permittivity of the guiding structure. In the case of dielectric waveguide we set

$$\varepsilon(x, z) = \varepsilon_{\text{bg}} + p[1 + \delta \sin(\omega_z z)] \exp(-x^2 / a^2), \quad (2)$$

where  $\varepsilon_{\text{bg}}$  is the relative background permittivity. The function (2) describes the profile of Gaussian waveguide with width  $a$  and depth  $p$ , which oscillates along the propagation direction with the amplitude  $\delta$  and frequency  $\omega_z$ . For convenience we denote dynamically varying part of dielectric permittivity as  $\delta \varepsilon_{\text{lin}}(x, z) = p \delta \sin(\omega_z z) \exp(-x^2 / a^2)$ .

In the absence of longitudinal modulation ( $\delta = 0$ ), all eigenmodes propagate independently and the power concentrated within each mode remains unchanged. Longitudinal permittivity modulation inside the waveguide couples different modes and stimulates energy exchange between them. Before we go to the numerical simulations of Eq. (1) and (2), it is instructive to consider the dynamics of this process using coupled-mode approach [6,23]. In this approach we use Lorentz reciprocity formula  $\nabla \cdot (\mathbf{H}_m \times \mathbf{E}_u^* + \mathbf{H}_u^* \times \mathbf{E}_m) = i\omega(\varepsilon_m - \varepsilon_u) \mathbf{E}_m \cdot \mathbf{E}_u^*$  that links the fields  $\{\mathbf{E}_m, \mathbf{H}_m\}$  in the waveguide with longitudinally modulated permittivity  $\varepsilon = \varepsilon_m$  with those  $\{\mathbf{E}_u, \mathbf{H}_u\}$  in the unmodulated guide with  $\varepsilon = \varepsilon_u$ , where  $\varepsilon_m - \varepsilon_u = \delta \varepsilon_{\text{lin}}$ . The field in the modulated waveguide can be represented as a superposition

$$\{\mathbf{E}_m, \mathbf{H}_m\} = \sum_n a_n(z) e^{i\beta_n z} \{\mathbf{E}^n, \mathbf{H}^n\}$$

of eigenmodes with  $z$ -dependent amplitudes  $a_n(z)$ . A similar representation can be used for  $\{\mathbf{E}_u, \mathbf{H}_u\}$  but with  $a_n = \text{const}$ . We substitute fields in such form into reciprocity formula, integrate it with respect to transverse coordinate  $x$ , and, taking into account the orthogonality condition  $\int \mathbf{e}_z \cdot (\mathbf{E}_n \times \mathbf{H}_k^*) dx = \delta_{nk}$ , arrive to the coupled-mode equations for amplitudes  $a_n(z)$ :

$$i \frac{da_n}{dz} = \sum_m \omega \mathcal{K}_{nm} a_m \exp[i(\beta_n - \beta_m)z], \quad (3)$$

where  $z$ -dependent coefficients  $\mathcal{K}_{nm}(z)$  are given by:

$$2\mathcal{K}_{nm} = \int \delta \varepsilon_{\text{lin}} (E_x^n E_x^{m*} + E_z^n E_z^{m*}) dx / \int \text{Re}(E_x^n H_y^{n*}) dx, \quad (4)$$

Taking into account variation of  $\delta \varepsilon_{\text{lin}} \sim \sin(\omega_z z)$  along the propagation distance, one can see that energy exchange between modes  $n$  and  $m$  will be most efficient if the resonance condition  $\beta_m - \beta_n \pm \omega_z = 0$  is satisfied, provided that the modes have the same symmetry, so that corresponding integral in the numerator of (4) is nonzero.

## 3. Numerical results and discussion

Rabi oscillations occur in multimode guiding structures. We search numerically for eigenmodes of the unmodulated ( $\delta = 0$ ) subwavelength Gaussian waveguide in the form  $\{\mathbf{E}(x, z), \mathbf{H}(x, z)\} =$

$\{\mathbf{E}^n(x), \mathbf{H}^n(x)\} \exp(i\beta_n z)$ . The components of vectors  $\mathbf{E}^n(x), \mathbf{H}^n(x)$  describe the transverse field distributions, while  $\beta_n$  are the propagation constants of the modes with indexes  $n=1, 2, \dots$ . We consider an illustrative situation when the waveguide supports three guided modes. This occurs for the following parameters:  $\varepsilon_{\text{bg}}=2.25$ ,  $p=2$ , and  $a=250$  nm. The width of the waveguide  $a$  is substantially smaller than the wavelength  $\lambda=632.8$  nm. The profiles of the transverse ( $E_x$ ) and longitudinal ( $E_z$ ) electric field components in all three guided modes are shown in Figs. 1(a) and 1(b), respectively. Modes are confined on the scale comparable with the wavelength  $\lambda$ . The longitudinal field component is comparable in amplitude with the transverse field one. The symmetry of Maxwell's equations dictates that  $E_z$  is antisymmetric for symmetric  $E_x$  and that the number of nodes in  $E_z$  always exceeds by one the number of nodes in  $E_x$ . In the following, when we mention the parity of the mode, we refer to the shape of the  $E_x$  component.

The propagation constants of the eigenmodes depicted in Figs. 1(a) and 1(b) are given by  $\beta_1 \approx 1.919k_0$ ,  $\beta_2 \approx 1.689k_0$ ,  $\beta_3 \approx 1.531k_0$ , where  $k_0 = \omega/c$  is the vacuum wavenumber. From the coupled mode equation [Eq. (3)], due to nonzero coefficient  $\mathcal{K}_{13}$ , the coupling is expected to occur for the first and third modes with equal parity at  $\omega_r = \beta_1 - \beta_3 \approx 0.389k_0$  that corresponds to a modulation period  $2\pi/\omega_r \approx 1.63$   $\mu\text{m}$ . Notice, that efficient coupling between first and second modes is impossible for symmetric permittivity perturbations  $\varepsilon(-x, z) = \varepsilon(x, z)$ , since corresponding coupling coefficient  $\mathcal{K}_{12}$  vanishes (coupling of these modes requires perturbations that break the symmetry of  $\varepsilon$ , such as transverse oscillations of the waveguide center).

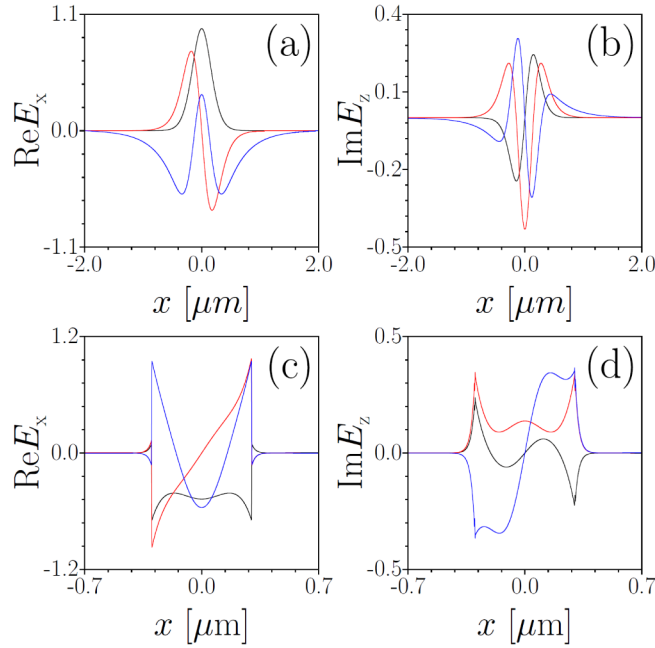


Fig. 1. Transverse (a) and longitudinal (b) electric field distributions in three linear eigenmodes of Gaussian waveguide with  $p=2$  and  $a=250$  nm. Transverse (c) and longitudinal (d) electric field distributions in three eigenmodes supported by the dielectric slab with  $a=600$  nm and  $p=2$  surrounded by metal with  $\text{Re}\varepsilon_m = -20$ .

The efficient coupling of the first and third modes of the subwavelength waveguide due to resonant ( $\omega_z = \omega_r$ ) longitudinal modulation is illustrated in Figs. 2(a) and 2(b). The results are obtained by direct solution of Maxwell's Eqs. (1) with finite-element method [24]. In Fig. 2(a) only the first mode was provided at the input, while in Fig. 2(b) only the third mode was provided. One can observe gradual transformation of the initial bell-shaped field distribution into three-hump distribution, characteristic for the third guided mode. In agreement with Eqs. (3), after accumulation of the power in the third mode, the reverse process starts and power flows

back into the first mode. This results in periodic Rabi oscillations having for  $\delta = 0.1$  the period as short as  $86 \mu\text{m}$ , irrespectively of the input mode index  $n$ .

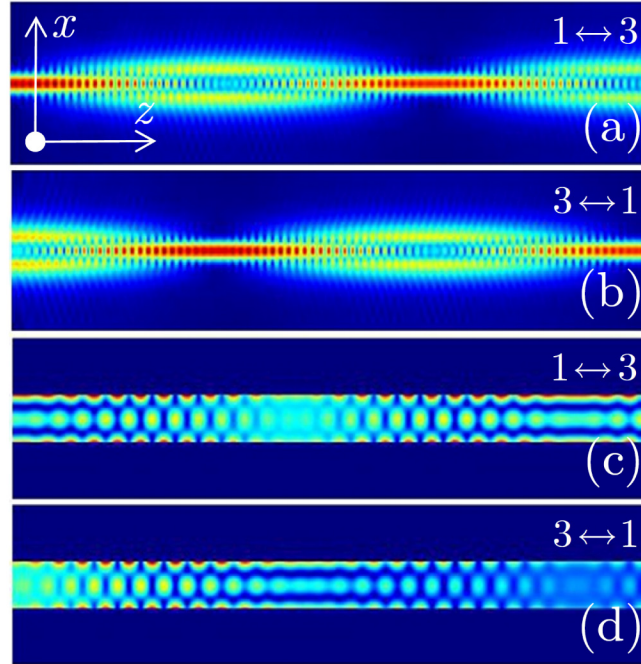


Fig. 2. (a),(b) Dynamic of resonant nonparaxial mode conversion at  $\delta = 0.1$  in dielectric structure at  $\omega_z = \omega_p \approx 0.389k_0$ , when only first or third mode is provided at the input. The propagation distance and transverse window size are  $130 \mu\text{m}$  and  $4 \mu\text{m}$ , respectively. (c),(d) Dynamics of mode conversion at  $\delta = 0.1$  and  $\omega_z = \omega_p \approx 0.232k_0$  in metal-dielectric-metal structure. The propagation distance and transverse window size are  $75 \mu\text{m}$  and  $2 \mu\text{m}$ , respectively. Only  $|E_x|^2$  distribution is shown.

The efficiency of mode conversion can be quantified using instantaneous weights of the modes  $\nu_n(z) = |c_n(z)|^2$ , where

$$c_n(z) = \int_{-\infty}^{\infty} E_x(x, z) H_y^{n*} dx / \int_{-\infty}^{\infty} E_x^n H_y^{n*} dx, \quad (5)$$

are the complex coefficients determining modal composition of the transverse component of the electric field  $E_x(x, z)$  at the distance  $z$ , while  $E_x^n(x)$ ,  $H_y^n(x)$  characterize field distributions in eigenmodes. The dependencies  $\nu_n(z)$  corresponding to dynamics from Figs. 2(a) and 2(b) are shown in Figs. 3(a) and 3(b). One can see that decrease in  $\nu_1$  is accompanied by the growth of the weight of the third mode  $\nu_3$  and vice versa, that indicates on resonant coupling of these two modes. At the same time, second mode is not excited and its weight  $\nu_2$  remains nearly zero. While modal field structure is in fact recovered after one period of oscillations, radiation and backward reflections, unavoidable for modulation depths  $\delta$  and periods  $2\pi/\omega_z$  considered here, slightly reduce the output quantity  $\nu_1 + \nu_2 + \nu_3$ . This circumstance is not accounted for by coupled-mode approach and can be captured only by solution of the full set of Maxwell's equations. Radiative losses rapidly decrease with decrease of  $\delta$ .

Stimulated mode conversion is the resonant effect. While in resonance nearly all power is transferred between modes, the efficiency of conversion drops down with increase of the detuning of modulation frequency from the resonant one. In Fig. 4(a) we show maximal weight of the third mode  $\nu_3^{\text{max}}$  acquired upon propagation as a function of the modulation frequency in the case, when only first mode is launched into structure at  $z = 0$ . The resonance is symmetric in  $\omega_z$  – its width depends on the depth of the longitudinal permittivity modulation. The width of the

resonance  $\delta\omega_z$ , defined at the level  $\nu_3 = \nu_3^{\max}/2$ , increases with  $\delta$  almost linearly [Fig. 4(b)]. For small  $\delta$  values resonant excitation of higher-order modes (in the case when structure supports several of them) can be made highly selective due to small resonance width. Another important quantity that characterizes the process considered here is the conversion length, or period of Rabi

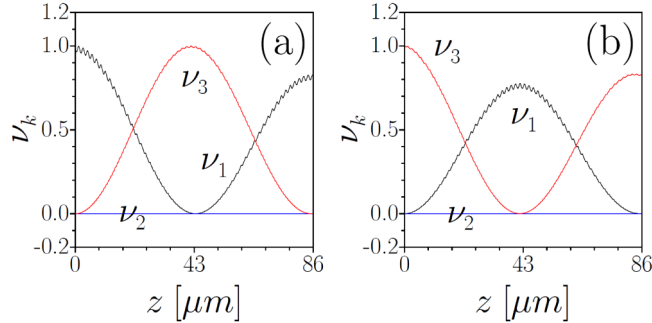


Fig. 3. Mode weights  $\nu_k = |c_k|^2$  versus propagation distance for  $1 \leftrightarrow 3$  and  $3 \leftrightarrow 1$  resonant transitions. The dependencies  $\nu_k(z)$  in (a),(b) correspond to evolution dynamics shown in Fig. 2.

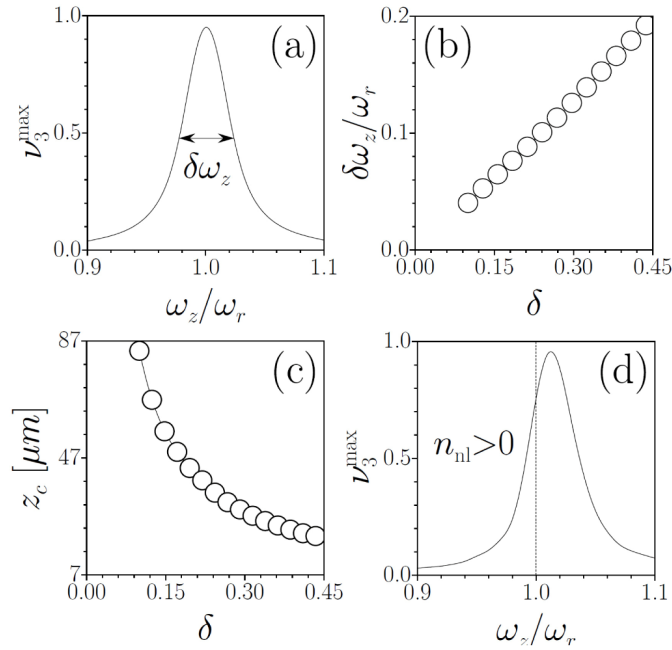


Fig. 4. (a) Maximal weight of the third mode versus modulation frequency at  $\delta = 0.1$  in the linear medium. Resonance width (b) and effective coupling distance at  $\omega_z = \omega_r$  (c) versus refractive index modulation depth  $\delta$  in the linear medium. (d) Maximal weight of the third mode versus modulation frequency in focusing medium for peak nonlinear contribution to the refractive index  $n_{nl} = 0.02$  and  $\delta = 0.1$ .

oscillations  $z_c$ , defined here as a distance at which most of the power returns back to the input eigenmode at  $\omega_z = \omega_r$ . In accordance with coupled-mode approach, where coupling distance evolves  $\sim 1/\mathcal{K}_{13}$ , with  $\mathcal{K}_{13} \sim \delta$ , one observes in Fig. 4(c) rapid decrease of  $z_c$  with increase of the permittivity modulation depth  $\delta$ . One should stress that in this structure the complete transformation of the shape of subwavelength light spots can be achieved at propagation distances as short as  $20 \mu\text{m}$ , provided that the permittivity modulation depth  $\delta$  is large enough.

So far, Rabi oscillations were considered only in dielectric guiding structures. The question arises whether similar effect can be observed in metal-dielectric waveguides, where the presence of metal allows to easily achieve light confinement at the subwavelength scales. We thus consider metal-dielectric-metal waveguide, whose permittivity is given by Eq. (2) for  $|x| \leq 300$  nm and by  $\varepsilon(x, z) = -20 - 0.19i$  (permittivity of silver at  $\lambda = 632.8$  nm) for  $|x| > 300$  nm. The shapes of eigenmodes of such a waveguide strongly differ from those in purely dielectric structures and the modes are more confined, but one still can see that the first and third modes are symmetric, while second mode is antisymmetric [Figs. 1(c) and 1(d)]. We found that despite losses in metal, the resonant longitudinal permittivity modulation in the dielectric region still results in efficient coupling between first and third modes in such a structure, as shown in Figs. 2(c) and 2(d).

Finally, Rabi oscillations are possible in the presence of focusing nonlinearity in the dielectric. We account for nonlinear response of the material by assuming that permittivity (2) includes an additional term  $\delta\varepsilon_{nl} = n_2(|E_x|^2 + |E_z|^2)$ , where  $n_2 > 0$  is the nonlinear coefficient. Solution of the Maxwell's Eqs. (1) reveals that weak focusing nonlinearity reduces the conversion length  $z_c$  [this is a direct consequence of the increase of the effective waveguide depth leading to growth of the overlap integral  $\mathcal{K}_{13}$  in (4)], and also shifts the exact resonance frequency to a higher value [Fig. 4(d)]. The latter fact can be explained taking into account that nonlinearity acts differently on propagation constants of eigenmodes, leading to higher growth of  $\beta_1$  in comparison with  $\beta_3$ , thereby increasing the difference  $\beta_1 - \beta_3$ . The nonlinear resonance curve becomes slightly asymmetric.

#### 4. Conclusion

In this paper, we have demonstrated that the Rabi oscillations are possible in various deeply subwavelength guiding structures (with widths down to 100 nm) including subwavelength dielectric waveguides and metal-dielectric-metal guiding structures, where the dynamics is governed by Maxwell's equations. Rabi oscillation for subwavelength modes may occur at very short propagation distances (about tens of microns), without considerable backward reflections, in both linear and nonlinear regimes. This enables controllable shaping of deeply subwavelength lights spots at extremely short distances.

#### Acknowledgments

The work of X. Zhang and F. Ye was supported by the National Natural Science Foundation of China (Grant No. 61475101 and 11104181).